Pergamon

Int. J. Solids Structures Vol. 33, No. 2, pp. 193–219, 1996

0020-7683/96 $9.50 + .00

0020-7683(95)00034-8

AXISYMMETRIC CRACK PROBLEM IN BONDED MATERIALS WITH A GRADED INTERFACIAL REGION

MURAT OZTURK and FAZIL ERDOGAN
Lehigh University, Bethlehem, PA 18015, U.S.A.

(*Received* 11 *September* 1994; *in revised form* 6 *February* 1995)

Abstract The problem of a penny-shaped crack in homogeneous dissimilar materials bonded through an interfacial region with graded mechanical properties is considered. The applied loads are assumed to be axisymmetric but otherwise arbitrary. The shear modulus of the interfacial region is assumed to be $\mu_2(z) = \mu_1 \exp(\alpha z)$ and that of the adherents μ_1 and $\mu_3 = \mu_1 \exp(\alpha h)$, h being the thickness of the region. A crack of radius a is located at the $z = 0$ plane. The axisymmetric mode III torsion problem is separated and treated elsewhere. Because of material nonhomogeneity, the deformation modes I and II considered in this study are always coupled. The related mixed boundary value problem is reduced to a system of singular integral equations. The asymptotic behavior of the stress state near the crack tip is examined, and the influence of the thickness ratio h/a and the material nonhomogeneity parameter α on the stress intensity factors and the strain energy release rate is investigated. The results show that the stress state near the crack tip would always have standard square-root singularity provided $h > 0$ or the material properties are continuous but not necessarily differentiable functions of z.

1. INTRODUCTION

In studying the fracture mechanics of bonded materials the structure and thickness of the interfacial regions seem to play an important role in determining the crack growth resistance parameters as well as the crack driving force. Very often, however, in such studies the interfacial region is simply neglected and the medium is assumed to be piecewise homogeneous. This type of simplified material model is generally adequate if the interfacial zone thickness is very small relative to the crack length and other macroscopic dimensions, and if the purpose is to evaluate, for example, the strain energy release rate as the measure of crack driving force [for review and references see Suo and Hutchinson (1990) and Rice *et al.* (1990)]. The model may be improved by assuming that the interfacial region consists of a relatively thin homogeneous layer with material properties different than that of the adjacent materials and the debonding crack is either embedded in the interfacial layer or lies along one of interfaces [see Arin and Erdogan (1971), Erdogan and Gupta (1971a, b), and Erdogan and Arin (1972) for bonded isotropic materials, and Erdogan and Wu (1993) for collinear interface cracks in orthotropic materials bonded through an orthotropic layer]. In using this particular homogeneous interfacial zone model for studying debonding fracture, even though such calculated fracture-related quantities as strain energy release rate, stress intensity factors and crack opening displacements are heavily influenced by the properties and the thickness of the interfacial layer, conceptually the related crack problems are the same as that of conventional embedded or interface cracks in piecewise homogeneous materials.

Recent studies, however, seem to indicate that largely as a consequence of material processing, in many cases the thermomechanical properties of the interfacial region vary continuously in thickness direction, resulting in a highly nonhomogeneous layer between two homogeneous materials. Electron microprobe line scans and scanning Auger depth profiles indeed show that in some diffusion bonded materials atomic composition of the two materials varies continuously across the nominal interface (Shiau *et al.*, 1988; Brennan, 1991). Similarly, during some deposition processes, as a consequence of sputtering there is a certain amount of mixing of the two species, giving again an interfacial region with steeply

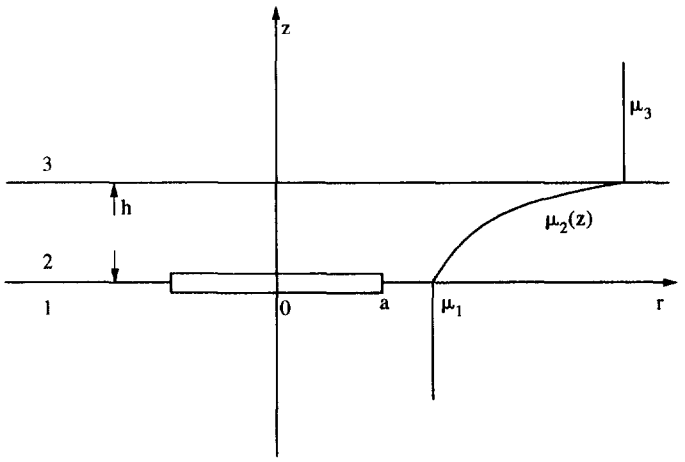

Fig. 1. The geometry of the problem for two dissimilar homogeneous materials bonded through a nonhomogeneous interfacial zone

graded properties (Batakis and Vogan, 1985; Houck *et al.*, 1987). There is also the new class of materials called 'Functionally Gradient Materials' (FGMs), used largely as coatings and interfacial zones, in which the material properties are intentionally graded. These are essentially two phase (e.g. metal/ceramic) nanocomposites synthesized in such a way that the volume fractions of the constituents vary continuously in thickness direction to give a predetermined composition profile [see Yamanouchi *et al.* (1990) and Holt *et al.* (1993) for extensive review and references]. FGM coatings and interfacial zones, designed mostly for high temperature applications, seem to be quite effective in reducing residual stresses resulting from processing (Lee and Erdogan, 1994) and in enhancing the bonding strength (Kerrihara *et al.*, 1990).

Fracture mechanics studies of bonded materials require the solution of certain standard crack problems. With the exception of two homogeneous half spaces bonded through an FGM layer containing a penny-shaped interface crack and subjected to torsion (Ozturk and Erdogan, 1995), the solution of few interface crack problems that exist in literature has been obtained under the assumption of plane strain (Delale and Erdogan, 1988a, b) or antiplane shear loading (Erdogan and Ozturk, 1992; Ozturk and Erdogan, 1993). In this study we consider the axisymmetric problem of two dissimilar elastic homogeneous half spaces bonded through a nonhomogeneous interfacial zone. Referring to Fig. 1, it is assumed that the composite medium contains a penny-shaped crack on one of the interfaces, the related mode III or the torsion problem has been uncoupled, and by separating the solution of the uncracked medium under given applied loads, the remaining coupled mode I–mode II problem is reduced to a perturbation problem in which the crack surface tractions σ_{zz} and σ_{rz} are the only nonzero external loads.

2. FORMULATION OF THE PROBLEM

The axisymmetric crack problem for the composite medium which consists of two homogeneous materials bonded through a nonhomogeneous interfacial region is described in Fig. 1. For each one of the constituents 1, 2 and 3 shown in Fig. 1, the kinematic relations, the Hooke's law and, in the absence of body forces, the equilibrium equations for the elastostatic problem may be expressed as follows:

$$\varepsilon_{irr} = \frac{\partial u_i}{\partial r}, \quad \varepsilon_{i\theta\theta} = \frac{u_i}{r}, \quad \varepsilon_{izz} = \frac{\partial w_i}{\partial z}, \quad 2\varepsilon_{irz} = \frac{\partial u_i}{\partial z} + \frac{\partial w_i}{\partial r}, \quad (i = 1, 2, 3) \tag{1}$$

$$\sigma_{irr} = (\lambda_i + 2\mu_i)\frac{\partial u_i}{\partial r} + \lambda_i\left(\frac{u_i}{r} + \frac{\partial w_i}{\partial z}\right),$$

$$\sigma_{i\theta\theta} = (\lambda_i + 2\mu_i)\frac{u_i}{r} + \lambda_i\left(\frac{\partial u_i}{\partial r} + \frac{\partial w_i}{\partial z}\right),$$

$$\sigma_{izz} = (\lambda_i + 2\mu_i)\frac{\partial w_i}{\partial z} + \lambda_i\left(\frac{\partial u_i}{\partial r} + \frac{u_i}{r}\right),$$

$$\sigma_{irz} = \mu_i\left(\frac{\partial u_i}{\partial z} + \frac{\partial w_i}{\partial r}\right), \quad (i = 1, 2, 3), \tag{2a–d}$$

$$\frac{\partial \sigma_{irr}}{\partial r} + \frac{\partial \sigma_{irz}}{\partial z} + \frac{1}{r}(\sigma_{irr} - \sigma_{i\theta\theta}) = 0, \tag{3a,b}$$

$$\frac{\partial \sigma_{irz}}{\partial r} + \frac{\partial \sigma_{izz}}{\partial z} + \frac{1}{r}\sigma_{irz} = 0, \quad (i = 1, 2, 3)$$

where in the usual notation λ_i and μ_i are Lamé's constants, u_i is the radial, w_i the axial component of the displacement vector, and ε_{ijk} and σ_{ijk}, respectively, refer to strains and stresses in the medium, $i = (1, 2, 3)$, $(j, k) = (r, \theta, z)$. In this study it is assumed that the Poisson's ratio of the composite medium is constant (i.e. $\nu_1 = \nu_2 = \nu_3 = \nu$) and the shear modulus μ_2 is approximated by

$$\mu_2(z) = \mu_1 e^{\alpha z}, \quad \alpha = \frac{1}{h}\log(\mu_3/\mu_1), \tag{4}$$

where h is the thickness of the interfacial layer and, depending on the relative magnitudes of μ_1 and μ_3, the constant α may be positive or negative. Even though it is based largely on mathematical expediency the foregoing assumption is not altogether unrealistic. The previous results as well as those obtained in this article indeed seem to show that in problems involving practical materials the influence of the Poisson's ratio on, for example, the stress intensity factors is rather insignificant (Delale and Erdogan, 1983; Konda and Erdogan, 1994). Also $\exp(\alpha z)$ is a convenient function to express steep material property variations in the interfacial zone in a simple manner. Furthermore, an exponentially varying modulus is quite adequate to study the basic features of the problem near the tip of a crack lying along a kink line of the material property distribution (Fig. 1).

Defining now $\kappa = 3 - 4\nu$ and substituting from eqns (1) and (2) into (3) we obtain

$$(\kappa+1)\left\{\frac{\partial^2 u_i}{\partial r^2} + \frac{1}{r}\frac{\partial u_i}{\partial r} - \frac{1}{r^2}u_i + \frac{\partial^2 w_i}{\partial r \partial z}\right\} + (\kappa-1)\alpha\left(\frac{\partial u_i}{\partial z} + \frac{\partial w_i}{\partial r}\right) + (\kappa-1)\left\{\frac{\partial^2 u_i}{\partial z^2} - \frac{\partial^2 w_i}{\partial r \partial z}\right\} = 0,$$

$$(\kappa+1)\left\{\frac{\partial^2 u_i}{\partial r \partial z} + \frac{1}{r}\frac{\partial u_i}{\partial z} + \frac{\partial^2 w_i}{\partial z^2}\right\} - (\kappa-1)\left\{\frac{\partial^2 u_i}{\partial r \partial z} - \frac{\partial^2 w_i}{\partial r^2}\right\}$$

$$- \frac{(\kappa-1)}{r}\left(\frac{\partial u_i}{\partial z} - \frac{\partial w_i}{\partial r}\right) + (3-\kappa)\alpha\left(\frac{\partial u_i}{\partial r} + \frac{u_i}{r}\right) + (\kappa+1)\alpha\frac{\partial w_i}{\partial z} = 0,$$

$$(\alpha = 0 \quad \text{for} \quad i = 1, 3; \quad \alpha \neq 0 \quad \text{for} \quad i = 2). \tag{5a,b}$$

Equations (5) must be solved under the following continuity, boundary and regularity conditions:

$$\left.\begin{aligned} u_3(r,z) &= u_2(r,z) \\ w_3(r,z) &= w_2(r,z) \end{aligned}\right\}, \quad 0 \leqslant r < \infty, \quad z = h, \tag{6}$$

$$\left.\begin{aligned} \sigma_{3zz}(r,z) &= \sigma_{2zz}(r,z) \\ \sigma_{3rz}(r,z) &= \sigma_{2rz}(r,z) \end{aligned}\right\}, \quad 0 \leqslant r < \infty, \quad z = h, \tag{7}$$

$$\left.\begin{aligned} \sigma_{2zz}(r,z) &= \sigma_{1zz}(r,z) \\ \sigma_{2rz}(r,z) &= \sigma_{1rz}(r,z) \end{aligned}\right\}, \quad 0 \leqslant r < \infty, \quad z = 0, \tag{8}$$

$$\left.\begin{aligned} \sigma_{1zz}(r,-0) &= \sigma_{2zz}(r,+0) = p_1(r) \\ \sigma_{1rz}(r,-0) &= \sigma_{2rz}(r,+0) = p_2(r) \end{aligned}\right\}, \quad 0 \leqslant r < a, \tag{9}$$

$$\left.\begin{aligned} u_1(r,-0) &= u_2(r,+0) \\ w_1(r,-0) &= w_2(r,+0) \end{aligned}\right\}, \quad a \leqslant r < \infty \tag{10}$$

$$u_i(r,z) \to 0, \quad w_i(r,z) \to 0. \quad \text{for} \quad r^2 + z^2 \to \infty, \quad (i = 1,2,3). \tag{11}$$

We now assume the solution of eqn (5) in the form

$$u_i(r,z) = \int_0^\infty F_i(z,\rho)\rho J_1(r\rho)\,\mathrm{d}\rho,$$

$$w_i(r,z) = \int_0^\infty G_i(z,\rho)\rho J_0(r\rho)\,\mathrm{d}\rho, \quad (i = 1,2,3) \tag{12a,b}$$

where J_0 and J_1 are the Bessel functions of the first kind. Substituting from eqn (12) into (5), defining $D = \mathrm{d}/\mathrm{d}z$, and inverting the related Hankel transforms we find

$$\{(\kappa-1)D^2 + \alpha(\kappa-1)D - (\kappa+1)\rho^2\}F_i - \{2\rho D + \alpha\rho(\kappa-1)\}G_i = 0,$$

$$\{2\rho D + \alpha(3-\kappa)\rho\}F_i + \{(\kappa+1)D^2 + \alpha(\kappa+1)D - (\kappa-1)\rho^2\}G_i = 0,$$

$$(\alpha = 0, \quad \text{for} \quad i = 1,3; \quad \alpha \neq 0, \quad \text{for} \quad i = 2). \tag{13a,b}$$

The solution of differential equations (13) may be expressed as

$$F_2(z,\rho) = \sum_{k=1}^{4} A_{k+2}(\rho)\,\mathrm{e}^{m_k z}, \quad G_2(z,\rho) = \sum_{k=1}^{4} B_{k+2}(\rho)\,\mathrm{e}^{m_k z}, \tag{14a,b}$$

with different sets of A_k, B_k and m_k for each medium, where A_k and B_k are unknown coefficients and $m_1, \ldots, m_4$ are the roots of the following characteristic equation:

$$m^4 + 2\alpha m^3 + (\alpha^2 - 2\rho^2)m^2 - 2\rho^2\alpha m + \frac{3-\kappa}{\kappa+1}\alpha^2\rho^2 + \rho^4 = 0. \tag{15}$$

From eqns (13) and (14) it can be shown that

$$B_{k+2} = a_k A_{k+2}, \tag{16}$$

$$a_k = -\frac{2\rho m_k + \rho\alpha(3-\kappa)}{(\kappa+1)m_k^2 + \alpha(\kappa+1)m_k - (\kappa-1)\rho^2}, \quad (k = 1, \ldots, 4). \tag{17}$$

The characteristic equation (14) may easily be expressed as

$$(m^2 + \alpha m - \rho^2)^2 + \frac{3-\kappa}{\kappa+1}\alpha^2\rho^2 = 0, \tag{18}$$

from which it follows that

$$m_1 = \bar{m}_3 = -\frac{\alpha}{2} + \frac{1}{2}\left\{\alpha^2 + \rho^2 + \mathrm{i}4\sqrt{\frac{3-\kappa}{\kappa+1}}\alpha\rho\right\}^{1/2},$$

$$m_2 = \bar{m}_4 = -\frac{\alpha}{2} - \frac{1}{2}\left\{\alpha^2 + \rho^2 + \mathrm{i}4\sqrt{\frac{3-\kappa}{\kappa+1}}\alpha\rho\right\}^{1/2} \tag{19a,b}$$

where bars refer to complex conjugates. After solving for $m_1, \ldots, m_4$, the expressions for coefficients a_k given by eqn (17) may be simplified as follows:

$$a_k = -\frac{2m_k + \alpha(3-\kappa)}{2\rho + \mathrm{i}\alpha\sqrt{(3-\kappa)(1+\kappa)}}, \quad (k = 1, 2), \quad a_3 = \bar{a}_1, \quad a_4 = \bar{a}_2. \tag{20a–c}$$

The foregoing derivation is for the nonhomogeneous material 2. For the homogeneous materials 1 and 3, by substituting $\alpha = 0$ in eqn (13), it may be shown that

$$F_i(\rho, z) = (A_{i1} + zA_{i2})\,\mathrm{e}^{\rho z} + (A_{i3} + zA_{i4})\,\mathrm{e}^{-\rho z},$$

$$G_i(\rho, z) = (B_{i1} + zB_{i2})\,\mathrm{e}^{\rho z} + (B_{i3} + zB_{i4})\,\mathrm{e}^{-\rho z}, \quad (i = 1, 3), \tag{21a,b}$$

$$B_{i1} = -A_{i1} + \frac{\kappa}{\rho}A_{i2}, \quad B_{i2} = -A_{i2},$$

$$B_{i3} = A_{i3} + \frac{\kappa}{\rho}A_{i4}, \quad B_{i4} = A_{i4}, \quad i = 1, 3. \tag{22a–d}$$

Using the regularity conditions (11) and defining the following new unknowns

$$A_1 = A_{11}, \quad A_2 = A_{12}, \quad A_7 = A_{33}, \quad A_8 = A_{34}, \tag{23a–d}$$

from eqns (21) and (22) it follows that

$$\left.\begin{aligned} F_1(\rho,z) &= (A_1+zA_2)\,e^{\rho z} \\ G_1(r,z) &= \left(-A_1+\left(\frac{\kappa}{\rho}-z\right)A_2\right)e^{\rho z} \end{aligned}\right\} z<0, \tag{24}$$

$$\left.\begin{aligned} F_3(\rho,z) &= (A_7+zA_8)\,e^{-\rho z} \\ G_3(r,z) &= \left(A_7+\left(\frac{\kappa}{\rho}+z\right)A_8\right)e^{-\rho z} \end{aligned}\right\} z>h. \tag{25}$$

By substituting now from eqns (14), (24) and (25) back into (12) and by using (2), the displacements and the relevant components of stresses may then be expressed as follows:

$$u_1(r,z) = \int_0^\infty (A_1+zA_2)\,e^{\rho z}\rho J_1(r\rho)\,d\rho,$$

$$w_1(r,z) = \int_0^\infty \left(-A_1+\left(\frac{\kappa}{\rho}-z\right)A_2\right)e^{\rho z}\rho J_0(r\rho)\,d\rho, \tag{26a,b}$$

$$u_2(r,z) = \int_0^\infty \sum_{k=1}^{4} A_{k+2}\,e^{m_k z}\rho J_1(r\rho)\,d\rho,$$

$$w_2(r,z) = \int_0^\infty \sum_{k=1}^{4} a_k A_{k+2}\,e^{m_k z}\rho J_0(r\rho)\,d\rho, \tag{27a,b}$$

$$u_3(r,z) = \int_0^\infty (A_7+zA_8)\,e^{-\rho z}\rho J_1(r\rho)\,d\rho,$$

$$w_3(r,z) = \int_0^\infty \left(A_7+\left(\frac{\kappa}{\rho}+z\right)A_8\right)e^{-\rho z}\rho J_0(r\rho)\,d\rho, \tag{28a,b}$$

$$\frac{1}{\mu_1}\sigma_{1zz} = \int_0^\infty \{-2\rho A_1+[\kappa+1-2\rho z]A_2\}\,e^{\rho z}\rho J_0(r\rho)\,d\rho,$$

$$\frac{1}{\mu_1}\sigma_{1rz} = \int_0^\infty \{2\rho A_1+[1-\kappa+2\rho z]A_2\}\,e^{\rho z}\rho J_1(r\rho)\,d\rho, \tag{29a,b}$$

$$\frac{\kappa-1}{\mu_2(z)}\sigma_{2zz} = \int_0^\infty \sum_{k=1}^{4} [(\kappa+1)m_k a_k+(3-\kappa)\rho]A_{k+2}\,e^{m_k z}\rho J_0(r\rho)\,d\rho,$$

$$\frac{1}{\mu_2(z)}\sigma_{2rz} = \int_0^\infty \sum_{k=1}^{4} [m_k-\rho a_k]A_{k+2}\,e^{m_k z}\rho J_1(r\rho)\,d\rho, \tag{30a,b}$$

$$\frac{1}{\mu_3}\sigma_{3zz} = \int_0^\infty \{-2\rho A_7-[\kappa+1+2\rho z]A_8\}\,e^{-\rho z}\rho J_0(r\rho)\,d\rho,$$

$$\frac{1}{\mu_3}\sigma_{3rz} = \int_0^\infty \{-2\rho A_7+[1-\kappa-2\rho z]A_8\}\,e^{-\rho z}\rho J_1(r\rho)\,d\rho. \tag{31a,b}$$

The functions $A_1,\ldots,A_8$ are determined from the boundary and the continuity conditions

of the problem. Equations (6)–(8) give the following six homogeneous algebraic equations in A_k:

$$\sum_{k=1}^{4} e^{m_k h} A_{k+2} - e^{-\rho h}(A_7 + hA_8) = 0,$$

$$\sum_{k=1}^{4} a_k e^{m_k h} A_{k+2} - e^{-\rho h}\left[A_7 + \left(\frac{\kappa}{\rho} + h\right)A_8\right] = 0,$$

$$\sum_{k=1}^{4} n_k e^{m_k h} A_{k+2} - e^{-\rho h}(\kappa - 1)[-2\rho A_7 - (\kappa + 1 + 2\rho h)A_8] = 0,$$

$$\sum_{k=1}^{4} l_k e^{m_k h} A_{k+2} - e^{-\rho h}[-2\rho A_7 + (1 - \kappa - 2\rho h)A_8] = 0,$$

$$\sum_{k=1}^{4} n_k A_{k+2} = (\kappa - 1)[-2\rho A_1 + (\kappa + 1)A_2],$$

$$\sum_{k=1}^{4} l_k A_{k+2} = 2\rho A_1 - (\kappa - 1)A_2, \tag{32a–f}$$

where

$$n_k = (3 - \kappa)\rho + (\kappa + 1)m_k a_k, \quad l_k = m_k - \rho a_k. \tag{33a,b}$$

Solving for $A_3, \ldots, A_8$, from eqns (32) it can be shown that

$$A_3 = (E_4 L_1 + E_6 \bar{L}_1)\hat{A}_1 + (E_4 L_2 + E_6 \bar{L}_2)\hat{A}_2,$$
$$A_4 = L_1 \hat{A}_1 + L_2 \hat{A}_2, \quad A_5 = \bar{A}_3, \quad A_6 = \bar{A}_4,$$
$$A_7 = \sum_{k=1}^{4}\left[1 + \frac{\rho h}{\kappa}(1 - a_k)\right] e^{(m_k + \rho)h} A_{k+2},$$
$$A_8 = \sum_{k=1}^{4} \frac{\rho}{\kappa}(a_k - 1)\, e^{(m_k + \rho)h} A_{k+2}, \tag{34a–f}$$

where the expressions for E_4, E_6, L_1 and L_2 are given in Appendix A, $\bar{L}_k$, $\bar{A}_{k+2}$ are the complex conjugates of L_k, A_{k+2}, $(k = 1, 2)$ and

$$\hat{A}_1 = 2\rho A_1, \quad \hat{A}_2 = (\kappa - 1)A_2. \tag{35}$$

The unknowns A_1 and A_2 may now be determined from the mixed boundary conditions (9) and (10).

3. THE DERIVATION OF INTEGRAL EQUATIONS

To reduce the mixed boundary conditions (9) and (10) to a system of integral equations we first define the following new unknown functions:

$$g_1(r) = \frac{\partial}{\partial r}\{w_2(r, +0) - w_1(r, -0)\},$$

$$g_2(r) = \frac{1}{r}\frac{\partial}{\partial r}\{ru_2(r, +0) - ru_1(r, -0)\}. \tag{36a,b}$$

From eqns (27), (28) and (30) it then follows that

$$g_1(r) = \int_0^\infty [(-1-2\rho Z_1)\rho A_1 + (\kappa-(\kappa-1)\rho Z_2)A_2]\rho J_1(r\rho)\,d\rho,$$

$$g_2(r) = \int_0^\infty [(-1+2\rho Y_1)\rho A_1 + (\kappa-1)\rho Y_2 A_2]\rho J_0(r\rho)\,d\rho, \tag{37a,b}$$

where the functions Z_i, Y_i, $(i = 1, 2)$ are defined in Appendix A. By taking the inverse transform of (37) and solving the resulting equations for A_1 and A_2 in terms of the new unknown functions g_1 and g_2 and observing that $g_k = 0$, $(k = 1, 2)$, for $r > a$, the functions A_1 and A_2 are found to be

$$\rho A_1 = \frac{(\kappa-1)\rho Y_2(\rho)}{\Delta_3(\rho)} \int_0^a s g_1(s) J_1(s\rho)\,ds - \frac{\kappa-(\kappa-1)\rho Z_2(\rho)}{\Delta_3(\rho)} \int_0^a s g_2(s) J_0(s\rho)\,ds.$$

$$A_2 = -\frac{2\rho Y_1(\rho)-1}{\Delta_3(\rho)} \int_0^a s g_1(s) J_1(s\rho)\,ds - \frac{(1+2\rho Z_1(\rho))}{\Delta_3(\rho)} \int_0^a s g_2(s) J_0(s\rho)\,ds, \tag{38a,b}$$

where

$$\Delta_3(\rho) = (\kappa-1)(-1-2\rho Z_1)\rho Y_2 - (-1+2\rho Y_1)(\kappa-(\kappa-1)\rho Z_2). \tag{39}$$

Up to this point all conditions of the problem except (9) have been used. Thus, by substituting from eqn (38) into (30), the conditions (9) may be expressed as

$$\int_0^\infty P_1(\rho)\rho J_0(r\rho)\,d\rho = \frac{1}{\mu_1} p_1(r), \quad 0 \leqslant r < a,$$

$$\int_0^\infty P_2(\rho)\rho J_1(r\rho)\,d\rho = \frac{1}{\mu_1} p_2(r), \quad 0 \leqslant r < a, \tag{40a,b}$$

where

$$P_1(\rho) = d_{11}(\rho) \int_0^a s g_1(s) J_1(s\rho)\,ds + d_{12}(\rho) \int_0^a s g_2(s) J_0(s\rho)\,ds,$$

$$P_2(\rho) = d_{21}(\rho) \int_0^a s g_1(s) J_1(s\rho)\,ds + d_{22}(\rho) \int_0^a s g_2(s) J_0(s\rho)\,ds, \tag{41a,b}$$

and the functions $d_{ij}(\rho)$, $(i, j = 1, 2)$ are also defined in Appendix A.

In order to avoid working with divergent kernels and to simplify the analysis regarding the asymptotic behavior of the kernels, first both sides of (40) are integrated in r. By using eqns (41) it may then be shown that

$$\int_0^r J_1(r\rho)\,d\rho \int_0^a (d_{11} J_1(\rho s) g_1(s) + d_{12} J_0(\rho s) g_2(s)) s\,ds = \frac{1}{\mu_1 r}\left(\int_0^r s p_1(s)\,ds + C_1\right),$$

$$-\int_0^r J_0(r\rho)\,d\rho \int_0^a (d_{21} J_1(\rho s) g_1(s) + d_{22} J_0(\rho s) g_2(s)) s\,ds = \frac{1}{\mu_1}\left(\int_0^r p_2(s)\,ds + C_2\right), \tag{42a,b}$$

where C_1 and C_2 are arbitrary constants. Equations (42) are essentially the integral equations that determine g_1 and g_2. For $\rho \to \infty$ it can be shown that the functions $d_{ij}(\rho)$ have the following asymptotic behavior:

$$d_{11}(\rho) = \frac{2}{\kappa - 1} + \frac{\kappa + 5}{2(\kappa + 1)^2}\left(\frac{\alpha}{\rho}\right) + \frac{(\kappa - 1)(\kappa - 3)}{4(\kappa + 1)^3}\left(\frac{\alpha}{\rho}\right)^2 + O(\rho^{-3}),$$

$$d_{12}(\rho) = \frac{1}{2(\kappa + 1)}\left(\frac{\alpha}{\rho}\right) + \frac{\kappa - 1}{4(\kappa + 1)^2}\left(\frac{\alpha}{\rho}\right)^2 + O(\rho^{-3}),$$

$$d_{21}(\rho) = -\frac{1}{2(\kappa + 1)}\left(\frac{\alpha}{\rho}\right) - \frac{\kappa - 1}{4(\kappa + 1)^2}\left(\frac{\alpha}{\rho}\right)^2 + O(\rho^{-3}),$$

$$d_{22}(\rho) = -\frac{2}{\kappa + 1} - \frac{1}{2(\kappa + 1)}\left(\frac{\alpha}{\rho}\right) - \frac{\kappa - 1}{4(\kappa + 1)^2}\left(\frac{\alpha}{\rho}\right)^2 + O(\rho^{-3}). \tag{43a–d}$$

Thus, from eqns (42) and (43) it may be shown that

$$\int_0^a \{(H_{11}(r,s) + h_{11}(r,s))g_1(s) + h_{12}(r,s)g_2(s)\}s\,\mathrm{d}s = \frac{\kappa + 1}{2\mu_1 r}\left(\int^r sp_1(s)\,\mathrm{d}s + C_1\right),$$

$$\int_0^a \{h_{21}(r,s)g_1(s) + (H_{22}(r,s) + h_{22}(r,s))g_2(s)\}s\,\mathrm{d}s = \frac{\kappa + 1}{2\mu_1}\left(\int^r p_2(s)\,\mathrm{d}s + C_2\right), \tag{44a,b}$$

where

$$H_{11}(r,s) = \int_0^\infty J_1(r\rho)J_1(s\rho)\,\mathrm{d}\rho = \frac{2}{\pi}\begin{cases} \dfrac{1}{s}[K(s/r) - E(s/r)], & s < r, \\ \dfrac{1}{r}[K(r/s) - E(r/s)], & s > r, \end{cases} \tag{45}$$

$$H_{22}(r,s) = \int_0^\infty J_0(r\rho)J_0(s\rho)\,\mathrm{d}\rho = \frac{2}{\pi}\begin{cases} \dfrac{1}{r}K(s/r), & s < r, \\ \dfrac{1}{s}K(r/s), & s > r, \end{cases} \tag{46}$$

$$h_{11}(r,s) = \int_0^\infty D_{11}(\rho)J_1(s\rho)J_1(r\rho)\,\mathrm{d}\rho,$$

$$h_{12}(r,s) = \int_0^\infty D_{12}(\rho)J_0(s\rho)J_1(r\rho)\,\mathrm{d}\rho,$$

$$h_{21}(r,s) = \int_0^\infty D_{21}(\rho)J_1(s\rho)J_0(r\rho)\,\mathrm{d}\rho,$$

$$h_{22}(r,s) = \int_0^\infty D_{22}(\rho)J_0(s\rho)J_0(r\rho)\,\mathrm{d}\rho, \tag{47a–d}$$

$$D_{11}(\rho)=\frac{d_{11}(\rho)}{d_{11}(\infty)}-1,\quad D_{12}(\rho)=\frac{d_{12}(\rho)}{d_{11}(\infty)},$$

$$D_{21}(\rho)=\frac{d_{21}(\rho)}{d_{22}(\infty)},\quad D_{22}(\rho)=\frac{d_{22}(\rho)}{d_{22}(\infty)}-1, \tag{48a–d}$$

$$d_{11}(\infty)=\frac{2}{\kappa+1},\quad d_{22}(\infty)=-\frac{2}{\kappa+1}, \tag{49a,b}$$

and K and E are, respectively, the complete elliptic integrals of the first and second kind defined by

$$K(k)=\int_0^{\pi/2}\frac{\mathrm{d}\theta}{(1-k^2\sin^2\theta)^{1/2}},\quad E(k)=\int_0^{\pi/2}(1-k^2\sin^2\theta)^{1/2}\,\mathrm{d}\theta,\quad 0\leqslant k\leqslant 1. \tag{50}$$

If equations (44) are differentiated term by term in r, the integral equations may be reduced to the following standard form:

$$\frac{1}{\pi}\int_0^a\left(\frac{1}{s-r}+\frac{1}{s+r}\right)g_1(s)\,\mathrm{d}s+\frac{1}{\pi}\int_0^a\sum_{j=1}^{2}m_{1j}(r,s)g_j(s)\,\mathrm{d}s=\frac{\kappa+1}{2\mu_1}p_1(r),$$

$$\frac{1}{\pi}\int_0^a\left(\frac{1}{s-r}-\frac{1}{s+r}\right)g_2(s)\,\mathrm{d}s+\frac{1}{\pi}\int_0^a\sum_{j=1}^{2}m_{2j}(r,s)g_j(s)\,\mathrm{d}s=\frac{\kappa+1}{2\mu_1}p_2(r), \tag{51a,b}$$

where the Fredholm kernels m_{ij} are given by

$$m_{11}(r,s)=\frac{M_1(r,s)-1}{s-r}+\frac{M_1(r,s)-1}{s+r}+\pi s\int_0^\infty D_{11}(\rho)\rho J_0(r\rho)J_1(s\rho)\,\mathrm{d}\rho,$$

$$m_{12}(r,s)=\pi s\int_0^\infty D_{12}(\rho)\rho J_0(r\rho)J_0(s\rho)\,\mathrm{d}\rho,$$

$$m_{21}(r,s)=-\pi s\int_0^\infty D_{21}(\rho)\rho J_1(r\rho)J_1(s\rho)\,\mathrm{d}\rho,$$

$$m_{22}(r,s)=\frac{M_2(r,s)-1}{s-r}-\frac{M_2(r,s)-1}{s+r}-\pi s\int_0^\infty D_{22}(\rho)\rho J_1(r\rho)J_0(s\rho)\,\mathrm{d}\rho, \tag{52a–d}$$

$$M_1(r,s)=\begin{cases}\dfrac{r}{s}E\left(\dfrac{s}{r}\right)+\dfrac{s^2-r^2}{rs}K\left(\dfrac{s}{r}\right), & s<r,\\[2ex] E\left(\dfrac{r}{s}\right), & s>r,\end{cases}$$

$$M_2(r,s)=\begin{cases}\dfrac{s}{r}E\left(\dfrac{s}{r}\right), & s<r,\\[2ex] \dfrac{s^2}{r^2}E\left(\dfrac{r}{s}\right)-\dfrac{s^2-r^2}{r^2}K\left(\dfrac{r}{s}\right), & s>r.\end{cases} \tag{53a,b}$$

From eqns (51) it may be seen that the dominant kernels of the integral equations are of the generalized Cauchy type (Erdogan, 1978). Thus by expressing the solution in the form

$$g_k(s) = \frac{f_k(s)}{(a-s)^{\eta_k}(a+s)^{\lambda_k}}, \quad -1 \leqslant \mathrm{Re}(\lambda_k, \eta_k) < 1, \quad (k = 1,2), \tag{54}$$

and using the function theoretic method described by Muskhelishvili (1953), the characteristic equations giving λ_k and η_k may be obtained as

$$\cot \pi\eta_k = 0, \quad (k = 1,2), \quad \cos \pi\lambda_1 = -1, \quad \cos \pi\lambda_2 = 1. \tag{55a–e}$$

The unknown functions f_1 and f_2 in eqn (54) are bounded in (0, a) and nonzero at $s = 0$ and $s = a$. In the penny-shaped crack shown in Fig. 1 physical considerations require that

$$[u_2(r,+0) - u_1(r,-0)] \to 0, \quad [w_2(r,+0) - w_1(r,-0)] \to 0, \quad \text{for} \quad r \to a,$$

$$u_2(r,+0) \to 0, \quad u_1(r,-0) \to 0, \quad \frac{\partial}{\partial r}[w_2(r,+0) - w_1(r,-0)] \to 0, \quad \text{for} \quad r \to 0. \tag{56}$$

From eqns (54)–(56) it then follows that the acceptable roots are

$$\eta_1 = \tfrac{1}{2}, \quad \eta_2 = \tfrac{1}{2}, \quad \lambda_1 = -1, \quad \lambda_2 = 0. \tag{57}$$

In addition to the standard parabolic behavior of the crack opening displacements near the crack tip $r = a$, eqns (30), (54) and (57) show that for small values of r we have

$$u^+ - u^- \simeq \frac{f_2(0)}{2\sqrt{a}} r, \quad w^+ - w^- \simeq w_0 + \frac{f_1(0)}{2\sqrt{a}} r^2, \quad r \ll a, \tag{58}$$

where w_0 is the total crack opening at $r = 0$. Referring to eqn (56) we also have $r(u^+ - u^-) = 0$ for $r = 0$ and $r = a$. Thus, the unknown function g_2 defined by eqn (51) must satisfy the following condition

$$\int_0^a r g_2(r)\, dr = 0. \tag{59}$$

It should be pointed out that for the interface crack problems in piecewise homogeneous materials (where the plane of the crack is a plane of material property discontinuity), the corresponding integral equations are of the second kind, having a Cauchy type kernel (Erdogan and Gupta, 1971b; Erdogan and Arin, 1972). As a result, the fundamental solution of the integral equations has complex singularities giving the well-known stress and displacement oscillations very near the crack tips. The results given in this study leading to eqns (54) and (57) indicate that the oscillatory behavior of stresses and displacements in crack problems for nonhomogeneous materials under modes I and II loading conditions would disappear if the material properties are continuous and not necessarily differentiable at and in the immediate vicinity of the crack tip [see also Delale and Erdogan (1988a)]. Furthermore, this result appears to be independent of the crack orientation. For example, similar results were found in plane strain and antiplane shear problems for a crack perpendicular to and terminating at the 'kink' line of the property distribution (Erdogan 1985; Erdogan *et al.* 1991; Martin 1992).

In order to avoid convergence difficulties that may be encountered in the numerical analysis, it is worthwhile to examine the Fredholm type kernels given in eqns (52) somewhat more closely. By observing that

$$\int_0^\infty J_1(a\rho)J_0(b\rho)\,d\rho = \begin{cases} 0, & a < b, \\ \dfrac{1}{a}, & a > b, \end{cases} \tag{60}$$

$$\int_0^\infty \frac{J_1(a\rho)J_0(b\rho)}{\rho}\,d\rho = \frac{2}{\pi}\begin{cases} E(b/a), & b < a, \\ \dfrac{b}{a}E(a/b) - \dfrac{b^2-a^2}{ab}K(a/b), & b > a, \end{cases} \tag{61}$$

$$\int_0^\infty \frac{J_1(a\rho)J_1(b\rho)}{\rho}\,d\rho = \frac{2}{\pi}\begin{cases} \dfrac{a}{2b}, & b < a, \\ \dfrac{b}{2a}, & b > a, \end{cases} \tag{62}$$

$$\int_0^\infty J_1(a\rho)J_1(b\rho)\,d\rho = H_{11}(a,b), \tag{63}$$

$$\int_0^\infty J_0(a\rho)J_0(b\rho)\,d\rho = H_{22}(a,b), \tag{64}$$

the expressions for m_{ij}, $(i,j = 1,2)$, given by eqn (52) may be written as

$$m_{11}(r,s) = \pi\gamma_1\begin{Bmatrix} 0, & s < r, \\ 1, & s > r, \end{Bmatrix} + \frac{M_1(r,s)-1}{s-r} + \frac{M_1(r,s)-1}{s+r}$$
$$+ 2\gamma_2 s M_1(r,s) + \pi s\int_0^\infty \hat{D}_{11}(\rho)\rho J_0(r\rho)J_1(s\rho)\,d\rho,$$

$$m_{12}(r,s) = \pi\beta_1 s H_{22}(r,s) + \pi s\int_0^\infty \hat{D}_{12}(\rho)\rho J_0(r\rho)J_0(s\rho)\,d\rho,$$

$$m_{21}(r,s) = -\pi\beta_1 s H_{11}(r,s) - \pi\beta_2\begin{Bmatrix} \dfrac{r}{2}, & s < r, \\ \dfrac{s^2}{2r}, & s > r, \end{Bmatrix} - \pi s\int_0^\infty \hat{D}_{21}(\rho)\rho J_1(r\rho)J_1(s\rho)\,d\rho,$$

$$m_{22}(r,s) = -\pi\beta_1\begin{Bmatrix} 0, & r < s, \\ \dfrac{s}{r}, & r > s, \end{Bmatrix} + \frac{M_2(r,s)-1}{s-r} - \frac{M_2(r,s)-1}{s+r}$$
$$- 2\beta_2 r M_2(r,s) - \pi s\int_0^\infty \hat{D}_{22}(\rho)\rho J_1(r\rho)J_0(s\rho)\,d\rho, \tag{65a–d}$$

where H_{11} and H_{22} are given by eqns (45) and (46) and

$$\hat{D}_{11}(\rho) = D_{11}(\rho) - \frac{\gamma_1}{\rho} - \frac{\gamma_2}{\rho^2}, \quad \hat{D}_{12}(\rho) = D_{12}(\rho) - \frac{\beta_1}{\rho},$$

$$\hat{D}_{21}(\rho) = D_{21}(\rho) - \frac{\beta_1}{\rho} - \frac{\beta_2}{\rho^2}, \quad \hat{D}_{22}(\rho) = D_{22}(\rho) - \frac{\beta_1}{\rho} - \frac{\beta_2}{\rho^2}, \tag{66a–d}$$

$$\gamma_1 = \frac{(\kappa+5)\alpha}{4(\kappa+1)}, \quad \gamma_2 = \frac{(\kappa-1)(\kappa-3)\alpha^2}{8(\kappa+1)}, \quad \beta_1 = \frac{\alpha}{4}, \quad \beta_2 = \frac{(\kappa-1)\alpha^2}{8(\kappa+1)}. \tag{67a-d}$$

From

$$\lim_{s\to r} \frac{M_i(r,s)-1}{s-r} = \lim_{s\to r} \frac{\mathrm{d}}{\mathrm{d}s} M_i(r,s), \quad (i=1,2), \tag{68}$$

and

$$\lim_{x\to 1} \{K(x) - \ln(4\sqrt{1-x^2})\} = 0, \tag{69}$$

it can now be shown that for small values of $|s-r|$ we have

$$\frac{M_1(r,s)-1}{s-r} \approx -\frac{1}{2r}\ln|s-r|, \quad \frac{M_2(r,s)-1}{s-r} \approx \frac{1}{2r}\ln|s-r|,$$
$$H_{11}(r,s) \approx \tfrac{1}{2}\ln|s-r|, \quad H_{22}(r,s) \approx \tfrac{1}{2}\ln|s-r|. \tag{70a-d}$$

That is, in addition to Cauchy type singularities, the kernels of the integral equations have logarithmic singularities which are square integrable and hence do not contribute to the singular behavior of the solution but have to be taken into account in the numerical analysis.

4. THE SOLUTION OF INTEGRAL EQUATIONS

The closed form solution of the integral equation (51) is not feasible. However, after obtaining the correct weight functions [as given by eqns (54) and (57)], the bounded unknown functions f_1 and f_2 may be determined to a desired degree of accuracy by expanding them into series of appropriate orthogonal polynomials and by regularizing the singular integral equations. If the interval is normalized by defining $y = (2s/a) - 1$, from eqns (54) and (57) it may be seen that the weight functions and the associated orthogonal polynomials become

$$\omega_1(y) = \sqrt{\frac{1+y}{1-y}}, \quad P_n^{(1,-1)}(y),$$
$$\omega_2(y) = \frac{1}{\sqrt{1-y}}, \quad P_n^{(1,0)}(y), \quad -1 < y < 1, \tag{71a,b}$$

where $P_n^{(\alpha,\beta)}(y)$, $(n = 0, 1, \ldots)$ are the Jacobi polynomials.

One may also develop an efficient technique by defining

$$g_1(as') = \phi_1(s')X_1(s'), \quad X_1(s') = \sqrt{\frac{s'}{1-s'}}, \quad s' = s/a, \tag{72}$$

$$g_2(as') = \phi_2(s')X_2(s'), \quad X_2(s') = \frac{1}{\sqrt{s'(1-s')}}, \quad s' = s/a, \tag{73}$$

and by requiring that $\phi_1(0) = 0$, $\phi_2(0) = 0$. The orthogonal polynomials associated with the weight functions X_1 and X_2 are seen to be (Appendix B)

$$P_n^{(1,2,1,2)}(t) = \frac{\Gamma(n+\frac{1}{2})}{n!\sqrt{\pi}} \frac{\cos(n+\frac{1}{2})\theta}{\cos\frac{\theta}{2}} = \frac{\Gamma(n+\frac{1}{2})}{n!\sqrt{\pi}} t_n(t),$$

$$P_n^{(1,2,-1,2)}(t) = \frac{\Gamma(n+\frac{1}{2})}{n!\sqrt{\pi}} \cos n\theta = \frac{\Gamma(n+\frac{1}{2})}{n!\sqrt{\pi}} T_n(t), \tag{74a,b}$$

$$(1+t)t_n(t) = T_n(t) + T_{n+1}(t), \quad t = 2s'-1 = \cos\theta, \quad -1 < t < 1. \tag{75a,b}$$

The unknown functions g_1 and g_2 may then be expressed as

$$\frac{2\mu_1}{\kappa+1} g_1(as') = \sqrt{\frac{s'}{1-s'}} \sum_0^{\infty} B_{1n} t_n(2s'-1),$$

$$\frac{2\mu_1}{\kappa+1} g_2(as') = \frac{1}{\sqrt{s'(1-s')}} \sum_0^{\infty} B_{2n} T_n(2s'-1), \tag{76a,b}$$

where B_{in} $(i = 1,2, n = 0,1,\ldots)$ are constant coefficients. In this article the weight functions and polynomials given by eqns (76) rather than (71) are used because of the simplicity of working with Chebyshev polynomials. Thus, by substituting from eqns (76) into the integral equations (51) and by observing that

$$\frac{1}{\pi}\int_0^1 \sqrt{\frac{s'}{1-s'}} \frac{t_n(2s'-1)\,ds'}{s'-r'} = \frac{1}{\pi}\int_{-1}^{1} \frac{T_n(t)+T_{n+1}(t)}{(t-x)\sqrt{1-t^2}}\,dt$$

$$= \begin{cases} U_{n-1}(x)+U_n(x), & |x|<1, \\ G_n(x)+G_{n+1}(x), & x>1, \end{cases} \tag{77}$$

$$x = 2r'-1, \quad r' = r/a, \quad U_n(x) = \frac{\sin(n+1)\theta}{\sin\theta}, \quad |x|<1, \quad \cos\theta = x,$$

$$G_n(x) = -\frac{(x-\sqrt{x^2-1})^n}{\sqrt{x^2-1}}, \quad x>1, \quad (n=0,1,\ldots), \tag{78a,b}$$

the integral equations may be reduced to the following system:

$$\sum_0^{\infty} \{F_{11j}(r')B_{1j} + F_{12j}(r')B_{2j}\} = p_1(ar'),$$

$$\sum_0^{\infty} \{F_{21j}(r')B_{1j} + F_{22j}(r')B_{2j}\} = p_2(ar'), \quad r' = r/a, \quad 0<r'<1, \tag{79a,b}$$

where

$$F_{11j}(r') = U_{j-1}(2r'-1) + U_j(2r'-1) - \frac{1}{2r'} W_j(2r'-1) + \gamma_1 v_j(r') + P_{11j}(r'),$$

$$F_{12j}(r') = -\beta_1 V_j(2r'-1) + P_{12j}(r'),$$

$$F_{21j}(r') = \beta_1 W_j(2r'-1) - \frac{\beta_2}{2}\left\{r' v_j(r') + \frac{e_{1j}(r')}{r'}\right\} + P_{21j}(r'),$$

$$F_{22j}(r') = 2U_{j-1}(2r'-1) + \frac{1}{2r'} V_j(2r'-1) - \frac{\beta_1}{r'} e_{2j}(r') + \gamma_1 v_j(r') + P_{22j}(r'), \tag{80a–d}$$

and

$$v_j(x) = \int_0^1 X_1(s)t_j(2s-1)\,ds,$$

$$e_{1j}(x) = \int_0^1 s^2 X_1(s)t_j(2s-1)\,ds,$$

$$e_{2j}(x) = \int_0^1 sX_2(s)T_j(2s-1)\,ds,$$

$$W_j(x) = \tfrac{1}{2}(V_j(x)+V_{j-1}(x)),$$

$$V_j(2r'-1) = \frac{1}{\pi}\int_0^1 \ln|s'-r'|X_2(s')T_j(2s'-1)\,ds', \tag{81a–e}$$

$$P_{11j}(r') = \frac{1}{\pi}\int_0^1 \left\{am_{11}(as',ar') + \frac{1}{2r'}\ln|s'-r'|\right\}X_1(s')t_j(2s'-1)\,ds',$$

$$P_{12j}(r') = \frac{1}{\pi}\int_0^1 \{am_{12}(as',ar') + \beta_1 \ln|s'-r'|\}X_2(s')T_j(2s'-1)\,ds',$$

$$P_{21j}(r') = \frac{1}{\pi}\int_0^1 \{am_{21}(as',ar') - \beta_1 \ln|s'-r'|\}X_1(s')t_j(2s'-1)\,ds',$$

$$P_{22j}(r') = \frac{1}{\pi}\int_0^1 \left\{am_{22}(as',ar') - \frac{1}{2r'}\ln|s'-r'|\right\}X_2(s')T_j(2s'-1)\,ds'. \tag{82a–d}$$

By substituting from eqn (76a) and by using the orthogonality condition for T_n, from eqn (59) we obtain

$$B_{20} + \tfrac{1}{2}B_{21} = 0. \tag{83}$$

Also, from eqns (72), (73) and (76), it may be seen that the conditions $\phi_1(0) = 0$ and $\phi_2(0) = 0$ become

$$\sum_{n=0}^{\infty}(-1)^n(2n+1)B_{1n} = 0, \quad \sum_{n=0}^{\infty}(-1)^n B_{2n} = 0. \tag{84}$$

The functional equations (79) may be solved by using a convenient method of weighted residuals. In this study a simple technique of collocation is used to reduce (79) to a system of linear algebraic equations (Kantorovitch and Krylov, 1958). In the numerical analysis the main questions which require careful consideration are the evaluation of the infinite integrals in the kernels $m_{ij}(r,s)$, the evaluation of the functions $P_{ijk}(r')$, $(i,j = 1,2,$ $k = 0,1,\ldots)$ given by eqn (83), and the question of the convergence of the series (76). Note that the integrals in (82) are all of Gauss–Jacobi type and may easily be evaluated by using the following quadrature formulas:

$$\int_{-1}^{1} h(\tau)(1-\tau^2)^{-1/2}\,d\tau \approx \frac{\pi}{M}\sum_{1}^{M} h(\tau_i), \quad T_M(\tau_i) = 0, \quad \tau_i = \cos\left(\frac{(2i-1)\pi}{2M}\right),$$

$$(i = 1,\ldots,M), \tag{85}$$

$$\int_{-1}^{1} h(\tau)\sqrt{\frac{1+\tau}{1-\tau}}\,d\tau \approx \frac{2\pi}{2M+1}\sum_{i=1}^{M}(1+\tau_i)h(\tau_i), \quad t_M(\tau_i)=0, \quad \tau_i=\cos\left(\frac{(2i-1)\pi}{2M+1}\right),$$

$$(i=1,\ldots,M). \quad (86)$$

Hence, the accuracy in the evaluation of the functions $P_{ijk}(r')$, $(i,j=1,2,k=0,1,\ldots)$ could easily be controlled by adjusting the number of terms in the Gauss–Jacobi sums.

It should be emphasized that the procedure described above is formal. To complete the analysis it is necessary to prove that the sequence of functions g_i^M obtained from eqns (76) by truncation will converge to the exact solutions g_i. For this, one has to prove that the sequences g_i^M are minimal or the related infinite system of algebraic equations is regular (Kantorovich and Krylov, 1958). The question of regularity for the problem under consideration seems to be very involved. For a special case, the proof that as $M\to\infty$, $g^M\to g$ is given by Erdogan and Gupta (1971c). To obtain the numerical results given in Section 7, M is increased until the repetition of four digits is observed in the calculated stress intensity factors. The largest number used was $M=16$.

5. STRESS INTENSITY FACTORS

From the viewpoint of applications of the results in fracture studies, one of the important quantities of interest is the strength of the stress singularity at the crack tips characterized by the stress intensity factors. We note that equations (51) give the stress components $\sigma_{1zz}(r,-0)$ and $\sigma_{1rz}(r,-0)$ outside as well as inside the region $(z=0, 0<r<a)$. Therefore, from eqn (51) one may easily obtain the stress intensity factors in terms of the unknown functions g_1 and g_2. The mode I and II stress intensity factors are defined by

$$k_1=\lim_{r\to a}\sqrt{2(r-a)}\sigma_{1zz}(r,-0), \quad k_2=\lim_{r\to a}\sqrt{2(r-a)}\sigma_{1rz}(r,-0). \quad (87a,b)$$

Since the functions

$$S_i(r)=\frac{1}{\pi}\int_0^a\sum_{j=1}^{2}m_{ij}(r,s)g_j(s)\,ds, \quad i=1,2 \quad (88)$$

are bounded in the closed interval $0\leqslant r\leqslant a$, eqns (51) may be expressed as

$$\frac{\kappa+1}{2\mu_1}\sigma_{1zz}(r,-0)=\frac{i}{\pi}\int_0^a\frac{\psi_1(s)}{(s-r)R_1^+(s)}\,ds+S_1(r),$$

$$\frac{\kappa+1}{2\mu_1}\sigma_{1rz}(r,-0)=\frac{i}{\pi}\int_0^a\frac{\psi_2(s)}{(s-r)R_2^+(s)}\,ds+S_2(r), \quad 0<r<\infty, \quad (89a,b)$$

where, referring to eqns (72) and (73),

$$\psi_1(s)=\phi_1(s,a), \quad \psi_2(s)=\phi_2(s/a), \quad (90)$$

$$R_1(z)=z^{-1/2}(z-a)^{1/2}, \quad R_1^+(r)=i\left(\frac{a-r}{r}\right)^{1/2},$$

$$R_2(z)=z^{1/2}(z-a)^{1/2}, \quad R_2^+(r)=i\sqrt{r(a-r)}$$

$$R_k^-(r)=-R_k^+(r), \quad (k=1,2). \quad (91a\text{–}c)$$

Consider now the following functions:

$$\Psi_k(z) = \frac{1}{2\pi i}\oint_C \frac{\psi_k(s)}{(s-z)R_k(s)}\,ds, \quad k = 1, 2, \tag{92}$$

where the contour C encircles the crack and z is outside C. By shrinking the contour to the cut, from eqns (89)–(92) we obtain

$$\frac{\kappa+1}{2\mu_1}\sigma_{1zz}(r, -0) = -\Psi_1(r) + S_1(r),$$

$$\frac{\kappa+1}{2\mu_1}\sigma_{2rz}(r, -0) = -\Psi_2(r) + S_2(r). \tag{93a,b}$$

On the other hand, following Muskhelishvili (1953), from eqn (92) it may be shown that

$$\Psi_i(z) = \frac{\psi_i(z)}{R_i(z)} - P_i(z), \quad (i = 1, 2), \tag{94}$$

where $P_i(z)$ is the principal part of $\psi_i(z)/R_i(z)$ at $z = \infty$. Thus, from eqns (92) and (94) we find

$$\frac{\kappa+1}{2\mu_1}\sigma_{1zz}(r, -0) = -\frac{\psi_1(r)}{R_1(r)} + P_1(r) + S_1(r),$$

$$\frac{\kappa+1}{2\mu_1}\sigma_{2rz}(r, -0) = -\frac{\psi_2(r)}{R_2(r)} + P_2(r) + S_2(r). \tag{95a,b}$$

From eqns (87), (90) and (95) it may now be seen that

$$k_1 = -\lim_{r\to a}\left(\frac{2\mu_1}{\kappa+1}\right)\sqrt{2(a-r)}\,q_1(r) = -\left(\frac{2\mu_1}{\kappa+1}\right)\sqrt{2a}\,\phi_1(1),$$

$$k_2 = -\lim_{r\to a}\left(\frac{2\mu_1}{\kappa+1}\right)\sqrt{2(a-r)}\,q_2(r) = -\left(\frac{2\mu_1}{\kappa+1}\right)\sqrt{2a}\,\phi_2(1). \tag{96a,b}$$

Or, by using eqns (76) the stress intensity factors are found to be

$$k_1 = -\sqrt{2a}\sum_0^c B_{1n}, \quad k_2 = -\sqrt{2a}\sum_0^c B_{2n}. \tag{97a,b}$$

For a homogeneous medium (i.e. for $\alpha = 0$ in eqn (4)) modes I and II crack problems are uncoupled and the stress intensity factors are given by

$$k_1 = -\frac{2}{\pi\sqrt{a}}\int_0^a \frac{rp_1(r)}{\sqrt{a^2-r^2}}\,dr, \quad k_2 = -\frac{2}{\pi a^{3/2}}\int_0^a \frac{r^2 p_2(r)}{\sqrt{a^2-r^2}}\,dr. \tag{98a,b}$$

In the limiting case of $h = 0$ the crack lies between two dissimilar materials 1 and 3. The system of singular integral equations (51) would then become

$$-\gamma g_2(r)+\frac{1}{\pi}\int_{-a}^{a}\frac{g_1(s)}{s-r}\,ds+\frac{1}{\pi}\int_{-a}^{a}K_1(r,s)g_1(s)\,ds=\frac{1}{\mu^*}p_1(r),$$

$$\gamma g_1(r)+\frac{1}{\pi}\int_{-a}^{a}\frac{g_2(s)}{s-r}\,ds+\frac{1}{\pi}\int_{-a}^{a}K_2(r,s)g_2(s)\,ds=\frac{1}{\mu^*}p_2(r), \tag{99a,b}$$

where

$$K_1(r,s)=\frac{M_1(|r|,|s|)-1}{s-r},\quad K_2(r,s)=\frac{M_2(|r|,|s|)-1}{s-r}. \tag{100a,b}$$

$$\mu^*=\mu_1\mu_3\frac{[(1+\kappa)\mu_3+(1+\kappa)\mu_1]}{(\mu_3+\mu_1\kappa)(\mu_1+\mu_3\kappa)},\quad \gamma=\frac{\mu_3(1-\kappa)-\mu_1(1-\kappa)}{(1+\kappa)\mu_3+(1+\kappa)\mu_1}. \tag{101a,b}$$

For an interface crack in piecewise homogeneous materials the stress intensity factors are defined by Erdogan and Arin (1972):

$$k_1+ik_2=\lim_{r\to a}\sqrt{2(a-r)}\left(\frac{r-a}{2a}\right)^{i\varepsilon}[\sigma_{zz}(r,0)+i\sigma_{rz}(r,0)],\quad \varepsilon=\frac{1}{2\pi}\log\left(\frac{1-\gamma}{1+\gamma}\right). \tag{102a,b}$$

In the special case of $\sigma_{zz}(r,0)=-p_0$, $\sigma_{rz}(r,0)=0$, $0\leqslant r<a$, for example, it may be shown that (Kassir and Bregman, 1972)

$$k_1+ik_2=2p_0\left(\frac{a}{\pi}\right)^{1/2}\frac{\Gamma(2+i\varepsilon)}{\Gamma(\frac{1}{2}+i\varepsilon)},\quad \varepsilon=\frac{1}{2\pi}\ln\left\{\frac{\mu_3+\mu_1\kappa}{\mu_1+\mu_3\kappa}\right\}. \tag{103a,b}$$

6. CRACK OPENING DISPLACEMENTS AND STRAIN ENERGY RELEASE RATE

After determining g_1 and g_2 or the coefficients B_{1n} and B_{2n} shown in eqns (76), the crack opening displacements may be obtained from eqns (36) as follows:

$$w_2(r,+0)-w_1(r,-0)=-\int_r^a g_1(s)\,ds=-\frac{a(\kappa+1)}{2\mu_1}$$
$$\times\left\{B_{10}(\theta'+\tfrac{1}{2}\sin 2\theta')+\sum_1^{\infty}B_{1n}\left(\frac{1}{2(n+1)}\sin(2n+2)\theta'+\frac{1}{2n}\sin 2n\theta'\right)\right\},$$

$$r[u_2(r,+0)-u_1(r,-0)]=-\int_r^a sg_2(s)\,ds=-\frac{a^2(\kappa+1)}{2\mu_1}\left\{B_{21}(\tfrac{1}{4}\sin 2\theta'+\tfrac{1}{8}\sin 4\theta')\right.$$
$$\left.+\sum_2^{\infty}B_{2n}\left(\frac{1}{2n}\sin 2n\theta'+\frac{1}{4n+4}\sin(2n+2)\theta'+\frac{1}{4n-4}\sin(2n-2)\theta'\right)\right\}, \tag{104a,b}$$

where

$$\cos^2\theta'=\frac{r}{a},\quad 0\leqslant r<a. \tag{105}$$

Note that $u_2(r,+0)-u_1(r,-0)$ vanishes for $r\to 0$. This may be seen from eqns (104b) and (73) by using the condition (55) as follows

$$\lim_{r\to 0}[u_2(r,+0)-u_2(r,-0)] = -\lim_{r\to 0}\frac{1}{r}\int_r^a sg_2(s)\,ds = -\lim_{r\to 0}\frac{d}{dr}\int_r^a sg_2(s)\,ds$$

$$= \lim_{r\to 0} r^{-\frac{1}{2}}\frac{\phi_2(r)}{\sqrt{r(a-r)}} = 0. \tag{106}$$

In debonding problems from the stand point of fracture mechanics, the strain energy release rate $\mathcal{G}$ is perhaps the most important parameter representing the magnitude of the applied loads and severity of component geometry. By using the concept of crack closure energy and the asymptotic behavior of stresses and displacements near the crack tip, $\mathcal{G}$ may be expressed as

$$\mathcal{G} = \frac{\pi(\kappa+1)}{8\mu_1}(k_1^2(a)+k_2^2(a)). \tag{107}$$

7. RESULTS AND DISCUSSION

The main results of this study are the stress intensity factors calculated for various loading conditions as functions of the material nonhomogeneity constant α defining the shear modulus in $\mu(z) = \mu_1 \exp(\alpha z)$ and h/a which is the basic dimensionless length parameter in the problem. Table 1 shows six different loading conditions used in the calculations. The table also shows the corresponding modes I and II stress intensity factors in a homogeneous medium containing a penny-shaped crack of radius a obtained from eqns (98). For the problem under consideration, some normalized stress intensity factors calculated for $\nu = 0.3$ are shown in Tables 2 and 3. Note that the results given in these tables may be used to obtain the stress intensity factors for arbitrary crack surface tractions by superposition to the extent that the tractions may be approximated by second degree polynomials in r. In all the results given in this section, the interfacial zone thickness h, the material nonhomogeneity parameter α, the variable r and the calculated quantities are normalized with respect to the crack radius a (Fig. 1). The results for $\alpha = 0$ shown in Tables 2 and 3 correspond to the stress intensity factors in a homogeneous medium shown in Table 1. It may be observed that as α increases, due to the increase in stiffness of the half space $z > 0$, the primary components of the stress intensity factors (i.e. k_1 due to the external loads p_0, p_1, p_2, and k_2 due to q_0, q_1, q_2) tend to decrease (Table 2). The table also shows that for all six loading conditions given in Table 1, secondary stress intensity factors are considerably smaller than the corresponding primary ones and, because of the uncoupling of deformation modes, vanish for $\alpha = 0$. For fixed values of the Poisson's ratio and αa the dependence of the stress intensity factors on the thickness ratio h/a is shown in Table 3. From $\mu_3 = \mu_1 \exp(\alpha h)$ and αa = constant it follows that for $h = 0$ the medium becomes homogeneous for which the stress intensity factors are given in Table 1. These results are seen to be the limits of the calculated stress intensity factors shown in Table 3 for $(h/a) \to 0$. However, for fixed μ_3/μ_1, in the limiting case of $h = 0$ the problem becomes one of bonded dissimilar half spaces containing a penny-shaped interface crack. As h/a approaches zero k_1 and k_2 do not tend to known limits that can be determined from the interface crack problem. For $(h/a) \to 0$, the quantity which remains continuous is the strain energy release rate $\mathcal{G} = \mathcal{G}(h)$ where $\mathcal{G}(h)$ is given by eqn (107) and $\mathcal{G}(0)$ is obtained from the solution of the interface crack problem in bonded dissimilar materials. Some representative sample results giving the calculated values of $\mathcal{G}(h)$ are shown in Fig. 2. The values of $\mathcal{G}(0)$ shown

Table 1. Loading conditions used and the corresponding stress intensity factors for $\alpha = 0$

$p_1(r)$	$-p_0$	$-p_1(r/a)$	$-p_2(r/a)^2$	0	0	0
$p_2(r)$	0	0	0	$-q_0$	$-q_1(r/a)$	$-q_2(r/a)^2$
k_1	$\frac{2}{\pi}p_0\sqrt{a}$	$\frac{2}{3}p_1\sqrt{a}$	$\frac{4}{3\pi}p_2\sqrt{a}$	0	0	0
k_2	0	0	0	$q_0\sqrt{a}$	$\frac{4}{3\pi}q_1\sqrt{a}$	$\frac{2}{5}q_2\sqrt{a}$

Table 2. The variation of stress intensity factors with αa for various loading conditions shown in Table 1. $\tau_i = p_i\sqrt{a}, \gamma_i = q_i\sqrt{a}, i = 0, 1, 2$

	$\sigma_{zz}(r,0) = p_1(r), \quad \sigma_{rz}(r,0) = 0, \quad \nu = 0.3, \quad h/a = 0.5$					
αa	k_1/τ_0	k_2/τ_0	k_1/τ_1	k_2/τ_1	k_1/τ_2	k_2/τ_2
−3.0	0.9052	−0.1396	0.6763	−0.0824	0.5532	−0.0542
−2.0	0.7946	−0.0813	0.6064	−0.0487	0.5018	−0.0327
−1.0	0.7065	−0.0358	0.5470	−0.0217	0.4596	−0.0149
−0.6	0.6764	−0.0204	0.5270	−0.0125	0.4450	−0.0086
−0.4	0.6624	−0.0133	0.5176	−0.0081	0.4377	−0.0056
−0.2	0.6492	−0.0065	0.5086	−0.0040	0.4309	−0.0028
−0.1	0.6428	−0.0032	0.5043	−0.0019	0.4276	−0.0014
0.0	0.6366	0.0	0.5	0.0	0.4244	0.0
0.1	0.6306	0.0031	0.4959	0.0019	0.4213	0.0013
0.2	0.6247	0.0062	0.4918	0.0038	0.4182	0.0027
0.4	0.6133	0.0121	0.4841	0.0075	0.4123	0.0053
0.6	0.6026	0.0177	0.4766	0.0109	0.4067	0.0077
1.0	0.5824	0.0284	0.4627	0.0176	0.3966	0.0125
2.0	0.5436	0.0506	0.4343	0.0318	0.3747	0.0230
3.0	0.5135	0.0684	0.4136	0.0436	0.3576	0.0319
	$\sigma_{zz}(r,0) = 0, \quad \sigma_{rz}(r,0) = p_2(r), \quad \nu = 0.3, \quad h/a = 0.5$					
αa	k_1/γ_0	k_2/γ_0	k_1/γ_1	k_2/γ_1	k_1/γ_2	k_2/γ_2
−3.0	0.0222	0.5503	0.0143	0.4530	0.0102	0.3953
−2.0	0.0156	0.5325	0.0103	0.4428	0.0074	0.3881
−1.0	0.0079	0.5157	0.0053	0.4333	0.0039	0.3814
−0.6	0.0047	0.5093	0.0032	0.4297	0.0024	0.3788
−0.4	0.0032	0.5061	0.0021	0.4279	0.0016	0.3775
−0.2	0.0016	0.5030	0.0011	0.4261	0.0007	0.3762
−0.1	0.0007	0.5015	0.0005	0.4253	0.0004	0.3756
0.0	0.0	0.5	0.0	0.4244	0.0	0.3750
0.1	−0.0007	0.4985	−0.0005	0.4236	−0.0004	0.3744
0.2	−0.0016	0.4970	−0.0011	0.4227	−0.0008	0.3738
0.4	−0.0031	0.4941	−0.0021	0.4210	−0.0016	0.3726
0.6	−0.0046	0.4912	−0.0032	0.4194	−0.0024	0.3714
1.0	−0.0076	0.4855	−0.0053	0.4161	−0.0040	0.3690
2.0	−0.0142	0.4725	−0.0104	0.4086	−0.0079	0.3636
3.0	−0.0205	0.4610	−0.0149	0.4018	−0.0116	0.3587

in Fig. 2 are calculated from the interface crack solution. The figure clearly shows that the function $\mathcal{G}(h)$ is continuous at $h = 0$. In the other limiting case of $h = \infty$, the medium becomes homogeneous having the shear modulus μ_1. We note that the normalizing strain energy release rate

$$\mathcal{G}_0 = \frac{\pi(1+\kappa)}{8\mu_1} p_0^2 a \tag{108}$$

used in Figs 2–4 is obtained for a pressurized crack of length $2a$ in a homogeneous medium under plane strain conditions, whereas the corresponding value for a penny-shaped crack of radius a is $(4/\pi^2)\mathcal{G}_0$, both for a unit crack front. Thus, for $(h/a) \to \infty$, $\mathcal{G}/\mathcal{G}_0$ would be expected to approach $4/\pi^2 = 0.4053$. This trend, too, may be observed in Fig. 2 for all values of μ_3/μ_1.

Some sample results showing the dependence of the strain energy release rate $\mathcal{G}$ as well as the stress intensity factors k_1 and k_2 on the modulus ratio μ_3/μ_1 are given in Figs 3 and 4. Note that for $\mu_3/\mu_1 = 1$ the medium is homogeneous and the corresponding stress intensity factors are shown in Table 1. In this case, from Table 1 and eqn (107) the normalized strain energy release rates for the loading conditions considered in Figs 3 and 4 may be obtained as $(4/\pi^2) = 0.4053$ and 0.25, respectively. The results for the special case of $\mu_3/\mu_1 = 1$ may easily be verified from Figs 3 and 4. As μ_3/μ_1 approaches zero, the stiffness of the half space $z > 0$ also approaches zero and, consequently, k_1, k_2 and $\mathcal{G}$ become unbounded. In the second limiting case of $(\mu_3/\mu_1) \to \infty$ the problem becomes one of an elastic material ($z < 0$) bonded to a rigid half space. Thus, as μ_3/μ_1 increases, as shown by the figures, k_1, k_2 and $\mathcal{G}$

Table 3. The variation of stress intensity factors with h/a for various loading conditions shown in Table 1

$\nu = 0.3, \quad \gamma a = 0.5$

h/a	$k_{11}/p_0\sqrt{a}$	$k_{12}/p_0\sqrt{a}$	$k_{21}/p_0\sqrt{a}$	$k_{22}/p_0\sqrt{a}$	$k_1/p_2\sqrt{a}$	$k_2/p_2\sqrt{a}$
0.0	0.6366	0	0.5000	0	0.4244	0
0.1	0.628	0.0052	0.494	0.0035	0.419	0.0027
0.2	0.621	0.0084	0.488	0.0055	0.415	0.0041
0.3	0.616	0.0110	0.485	0.0071	0.413	0.0051
0.4	0.6117	0.0132	0.4827	0.0083	0.4109	0.0059
0.5	0.6079	0.0149	0.4803	0.0092	0.4093	0.0065
0.6	0.6046	0.0164	0.4783	0.0100	0.4079	0.0070
0.7	0.6018	0.0177	0.4767	0.0107	0.4068	0.0074
0.8	0.5993	0.0186	0.4753	0.0112	0.4058	0.0078
0.9	0.5973	0.0195	0.4741	0.0117	0.4051	0.0081
1.0	0.5955	0.0201	0.4731	0.0120	0.4044	0.0083
2.0	0.5873	0.0226	0.4683	0.0135	0.4012	0.0092
3.0	0.5852	0.0230	0.4670	0.0137	0.4004	0.0094
4.0	0.5845	0.0231	0.4666	0.0137	0.4001	0.0094
5.0	0.5842	0.0231	0.4665	0.0137	0.4000	0.0094

h/a	$k_{11}/q_0\sqrt{a}$	$k_{12}/q_0\sqrt{a}$	$k_{21}/q_0\sqrt{a}$	$k_{22}/q_0\sqrt{a}$	$k_1/q_2\sqrt{a}$	$k_2/q_2\sqrt{a}$
0.0	0	0.5000	0	0.4244	0	0.3750
0.1	0.002	0.497	0.0017	0.423	0.0014	0.374
0.2	0.003	0.495	0.0025	0.422	0.0019	0.373
0.3	0.004	0.494	0.0027	0.421	0.0021	0.3727
0.4	0.0039	0.4933	0.0028	0.4201	0.0021	0.3723
0.5	0.0038	0.4926	0.0027	0.4202	0.0020	0.3719
0.6	0.0036	0.4921	0.0025	0.4198	0.0018	0.3717
0.7	0.0033	0.4916	0.0023	0.4195	0.0017	0.3715
0.8	0.0030	0.4912	0.0021	0.4192	0.0015	0.3713
0.9	0.0027	0.4909	0.0018	0.4190	0.0014	0.3712
1.0	0.0025	0.4907	0.0017	0.4189	0.0013	0.3711
2.0	0.0013	0.4899	0.0009	0.4184	0.0007	0.3707
3.0	0.001	0.4898	0.0007	0.4184	0.0005	0.3707
4.0	0.001	0.4898	0.0007	0.4184	0.0005	0.3707
5.0	0.001	0.4898	0.0007	0.4184	0.0005	0.3707

approach certain finite limits. The figures also show that at $(\mu_3/\mu_1) = 1$, as expected, the secondary stress intensity factors change sign. The physical consequence of this may be the change of sign of the probable crack growth angle θ_0 shown in Fig. 5 which is calculated from (Erdogan and Sih, 1963)

$$k_1 \sin\theta_0 + k_2(3\cos\theta_0 - 1) = 0, \quad \sigma_{\theta\theta}(r, \theta_0) > 0. \tag{109}$$

The figure shows that if the medium is isotropic with regard to the crack growth resistance $\mathcal{G}_c$, the maximum energy release and, as a result further crack growth, would take place in a direction toward the less stiff material. On the other hand, if $\mathcal{G}_c = \mathcal{G}_c(\theta)$, then the crack growth direction θ_0 would be such that $\mathcal{G}(\theta)/\mathcal{G}_c(\theta)$ is maximum, $\mathcal{G}(\theta)$ being the energy release rate for a small radial crack extension in the direction of θ.

In this study, largely to simplify the analysis, the Poison's ratio ν is assumed to be constant. In an actual nonhomogeneous medium this, of course, is not possible. The assumption can only be justified if the fracture mechanics parameters of interest, in this case the stress intensity factors, prove to be relatively insensitive to variations in the Poisson's ratio. To give some idea about the influence of the variations in ν on the stress intensity factors, some additional results are given in Table 4. The table shows the normalized stress intensity factors for various values of ν and for fixed values of h/a and μ_3/μ_1. The external loads used are also shown in the tables. It may be observed that the influence

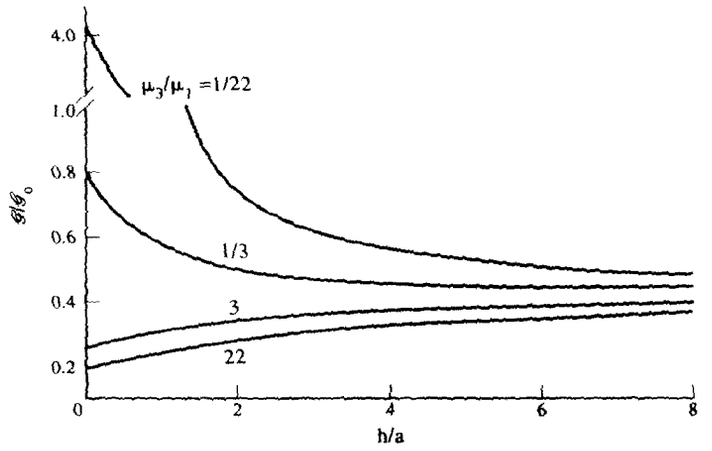

Fig. 2. Variation of strain energy release rate with h/a for $\nu = 0.3$, and $\sigma_{1zz} = -p_0$, $\sigma_{1rz} = 0$, $\mathscr{G}_0 = \pi(1+\kappa)p_0^2 a/8\mu_1$.

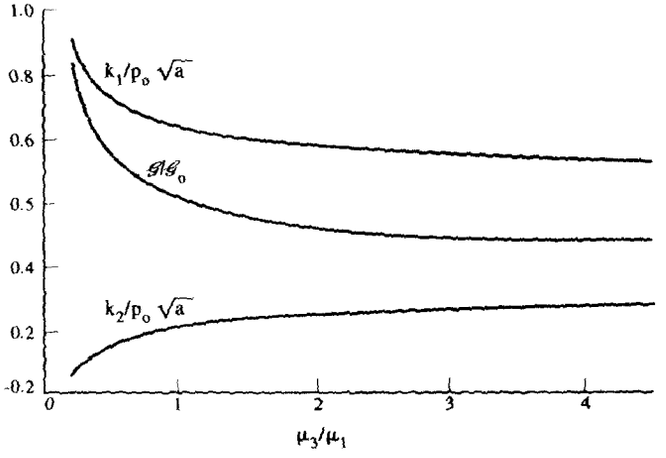

Fig. 3. Variation of stress intensity factors and strain energy release rate with stiffness ratio μ_3/μ_1; $\nu = 0.3$, $h/a = 0.5$, $\sigma_{1zz} = -p_0$, $\sigma_{1rz} = 0$, $\mathscr{G}_0 = \pi(1+\kappa)p_0^2 a/8\mu_1$.

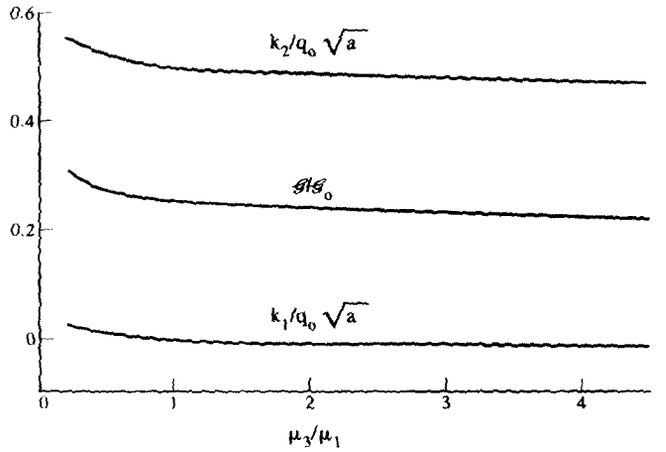

Fig. 4. Variation of stress intensity factors and strain energy release rate with stiffness ratio μ_3/μ_1; $\nu = 0.3$, $h/a = 0.5$, $\sigma_{1zz} = 0$, $\sigma_{1rz} = -q_0$, $\mathscr{G}_0 = \pi(1+\kappa)q_0^2 a/8\mu_1$.

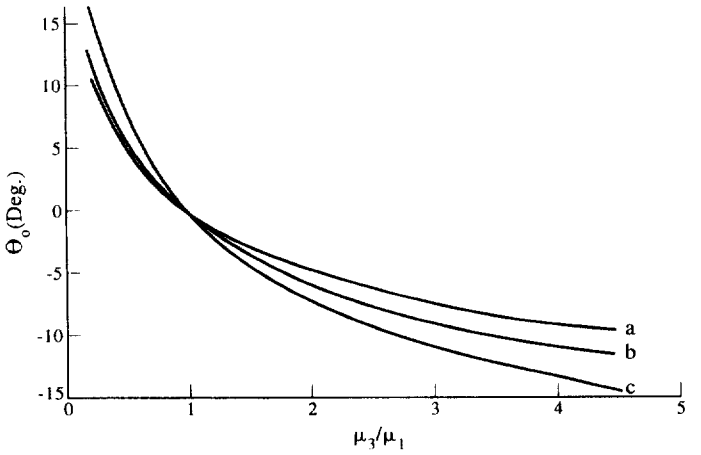

Fig. 5. The probable crack growth direction θ_0 vs μ_3/μ_1 for $h/a = 0.5$, $\nu = 0.3$, $\sigma_{zz}(r,0) = 0$, (a) $\sigma_{zz}(r,0) = -p_2(r/a)^2$, (b) $\sigma_{zz}(r,0) = -p_1(r/a)$, (c) $\sigma_{zz}(r,0) = -p_0$.

Table 4. The influence of the Poisson's ratio on the stress intensity factors, loading: $\sigma_{zz}(r,0) = (-p_0, -p_1(r/a), -p_2(r/a)^2)$, $\sigma_{rz}(r,0) = 0$, $0 \leqslant r < a$

ν	$\frac{k_1}{p_0\sqrt{a}}$	$\frac{k_2}{p_0\sqrt{a}}$	$\frac{k_1}{p_1\sqrt{a}}$	$\frac{k_2}{p_1\sqrt{a}}$	$\frac{k_1}{p_2\sqrt{a}}$	$\frac{k_2}{p_2\sqrt{a}}$
			$\mu_3/\mu_1 = 1.22$, $h/a = 0.5$			
0.01	1.278	−0.459	0.902	−0.255	0.714	−0.149
0.1	1.316	−0.466	0.926	−0.260	0.731	−0.155
0.2	1.363	−0.471	0.955	−0.265	0.751	−0.159
0.3	1.418	−0.472	0.989	−0.267	0.774	−0.164
0.4	1.487	−0.465	1.032	−0.264	0.806	−0.168
0.5	1.574	−0.436	1.086	−0.252	0.845	−0.169
			$\mu_3/\mu_1 = 22$, $h/a = 0.5$			
0.01	0.445	0.145	0.366	0.094	0.320	0.073
0.1	0.450	0.134	0.369	0.087	0.322	0.068
0.2	0.455	0.122	0.371	0.079	0.323	0.061
0.3	0.459	0.105	0.372	0.069	0.324	0.054
0.4	0.460	0.084	0.372	0.056	0.323	0.043
0.5	0.456	0.056	0.367	0.039	0.318	0.029

of the Poisson's ratio on the stress intensity factors does not seem to be very significant. The exception appears to be the case of relatively large negative values of αa or very small values of μ_3/μ_1 in cracks under mode I loading.

An example showing the relative crack opening in z direction, $w_2^+ - w_1^-$ is given in Fig. 6 where the normalization factor w_0 is the maximum relative crack surface displacement for the corresponding pressurized plane strain crack in a homogeneous medium. Note that for $(\mu_3/\mu_1) = 1$ the displacement amplitudes for the axisymmetric and plane strain cracks differ by a factor of $(2\pi) = 0.6366$. The results shown in Fig. 6 are calculated from eqn (104a).

The results given in this article and the more extensive results given by Ozturk and Erdogan (1994) show the effect of composition grading and the thickness of the interfacial zones on certain fracture mechanics parameters. They can be used by material scientists as an additional screening tool in optimizing the material design. They can also be used by design and maintenance engineers in modeling the subcritical crack growth process needed for service life estimates.

Acknowledgements This research was supported by the AFOSR, Grant F49620-93-1-0252 and the NSF Grant MSS-9114439. The authors would also like to acknowledge the summer support provided by the ONR Grant N0014-93-1-0557.

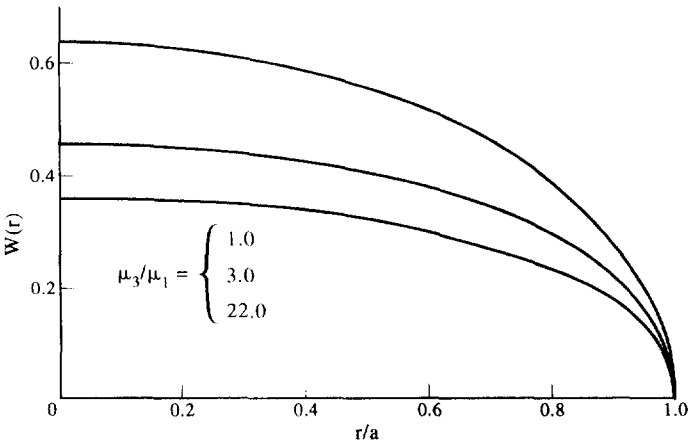

Fig. 6. z-Component of the normalized crack opening displacement, $W = (w_2 - w_1)/w_0$, $w_0 = (1+\kappa)p_0 a/2\mu_1$; $\nu = 0.3$, $h/a = 0.4$, $\sigma_{1zz}(r,0) = -p_0$, $\sigma_{rz}(r,0) = 0$, $0 \leqslant r < a$.

REFERENCES

Abramowitz, M. and Stegun, I. A. (1972). *Handbook of Mathematical Functions*, Dover Publications, New York.

Arin, K. and Erdogan, F. (1971). Penny-shaped crack in an elastic layer bonded to dissimilar half spaces. *Int. J. Engng Sci.* **9**, 213–232.

Batakis, A. P. and Vogan, J. W. (1985). Rocket thrust chamber thermal barrier coatings. NASA CR-1750222.

Brennan, J. J. (1991). Interfacial studies of refractory glass ceramic matrix/advanced SiC fiber reinforced composites. Annual Report, ONR Contract N00014-87-C-0699, United Technologies Research Center.

Comninou, M. (1977). The interface crack. *ASME J. Appl. Mech.* **44**, 631–636.

Delale, F. and Erdogan, F. (1983). The crack problem for a nonhomogeneous plane. *ASME J. Appl. Mech.* **50**, 609–614.

Delale, F. and Erdogan, F. (1988a). Interface crack in a nonhomogeneous elastic medium. *Int. J. Engng Sci.* **28**, 559–568.

Delale, F. and Erdogan, F. (1988b). On the mechanical modeling of the interfacial regions in bonded materials. *ASME J. Appl. Mech.* **55**, 317–324.

Erdogan, F. (1978). Mixed boundary value problems in mechanics. *Mech. Today* **4**, 1–86.

Erdogan, F. (1985). The crack problem for bonded nonhomogeneous materials under antiplane shear loading. *ASME J. Appl. Mech.* **52**, 823–828.

Erdogan, F. and Arin, K. (1972). Penny-shaped interface crack between an elastic layer and a half space. *Int. J. Engng Sci.* **10**, 115–125.

Erdogan, F. and Gupta, G. D. (1971a). The stress analysis of multi-layered composites with a flaw. *Int. J. Solids Structures* **7**, 39–61.

Erdogan, F. and Gupta, G. D. (1971b). Layered composites with an interface flaw. *Int. J. Solids Structures* **7**, 1089–1107.

Erdogan, F. and Gupta, G. D. (1971c). The problem of an elastic stiffener bonded to a half plane. *ASME J. Appl. Mech.* **38**, 937–942.

Erdogan, F. and Ozturk, M. (1992). Diffusion problems in bonded nonhomogeneous materials. *Int. J. Engng Sci.* **30**, 1507–1523.

Erdogan, F. and Sih, G. C. (1963). On the crack extension in plates under plane loading and transverse shear. *J. Basic Engng. Trans. ASME* **85**, 519–525.

Erdogan, F. and Wu, B. H. (1993). Interface crack problems in layered orthotropic materials. *J. Mech. Phys. Solids* **41**, 889–917.

Erdogan, F., Kaya, A. C. and Joseph, P. F. (1991). The crack problem in bonded nonhomogeneous materials. *ASME J. Appl. Mech.* **58**, 410–418.

Holt, J. B., Koizumi, M., Hirai, T. and Munir, Z. A. (eds) (1993). *Ceramic Transactions—Functionally Gradient Materials*, Vol. 34. American Ceramic Society, Westerville, OH.

Houck, D. L. (ed.) (1987). *Thermal Spray—Advances in Coatings Technology, Proceeding of the National Thermal Spray Conference*, Orlando, FL. ASM International.

Kantorovich, L. V. and Krylov, V. I. (1958). *Approximate Methods of Higher Analysis*. Wiley Interscience, New York.

Kassir, M. K. and Bregman, A. M. (1972). The stress intensity factor for a penny-shaped crack between two dissimilar materials. *J. Appl. Mech.* **39**, *Trans. ASME*, 94, *Series E*, 308–310.

Konda, N. and Erdogan, F. (1994). The mixed-mode crack problem in a nonhomogeneous elastic medium. *Engng Fracture Mech.* **47**, 533–545.

Kurihara, K., Sasaki, K. and Kawarada, M. (1990). Adhesion improvement of diamond films. FGM-90, *Proc. 1st Int. Symp. on Functionally Gradient Materials*. (Edited by M. Yamanouchi, M. Koizumi, T. Hirai and I. Shiota). FGM Forum, Sendai, Japan.

Lee, Y. D. and Erdogan, F. (1995). Residual stresses in FGM and laminated thermal barrier coatings. *Int. J. Fracture* **69**, 145–165.

Martin, P. A. (1992). Tip behavior for cracks in bonded inhomogeneous materials. *J. Engng Mathemat.* **26,** 467–480.
Muskhelishvili, I. N. (1953). *Singular Integral Equations*. P. Noordhoff, Groningen, Holland.
Ozturk, M. and Erdogan, F. (1993). Antiplane shear crack problem in bonded materials with a graded interfacial zone. *Int. J. Engng Sci.* **31,** 1641–1657.
Ozturk, M. and Erdogan, F. (1994). Axisymmetric crack problem in bonded materials with a graded interfacial region. Technical Report, AFOSR Grand F49620-93-1-0252.
Ozturk, M. and Erdogan, F. (1995). An axisymmetric crack in bonded materials with a nonhomogeneous interfacial zone under torsion. *ASME J. Appl. Mech.* **62,** 116–125.
Rice, J. R., Suo, Z. and Wang, J. S. (1990). Mechanics and thermodynamics of brittle interfacial failure in bimaterial systems. *Metal Ceramic Interfaces* (Edited by M. Rühle, A. G. Evans, M. F. Ashley and J. Hirth), pp. 269–294. Pergamon Press, Oxford.
Shiau, F. Y., Zuo, Y., Zeng, X. Y., Lin, J. C. and Chang, Y. A. (1988). Interfacial reactions between copper and GaAs. *Adhesion in Solids*, Materials Research Society Symposium Proc., Vol. 119 (Edited by D. M. Mattox, J. E. E. Baglin, R. J. Gottshall and C. D. Batich), pp. 171–176. MRS, Pittsburgh, PA.
Suo, Z. and Hutchinson, J. W. (1990). Interface crack between two elastic layers. *Int. J. Fracture* **43,** 1–18.
Yamanouchi, M., Koizumi, M., Hirai, T. and Shiota, I. (eds) (1990). FGM-90, *Proc. 1st Int. Symp. on Functionally Gradient Materials*. FGM Forum, Sendai, Japan.

APPENDIX A

Expressions for various functions that appear in Section 3

$$Z_1(\rho) = a_1 H_1 + \bar{a}_1 \bar{H}_1 + a_2 L_1 + \bar{a}_2 \bar{L}_2 \tag{A1}$$

$$Z_2(\rho) = a_1 H_2 + \bar{a}_1 \bar{H}_2 + a_2 L_2 + \bar{a}_2 \bar{L}_2 \tag{A2}$$

$$Y_1(\rho) = H_1 + \bar{H}_1 + L_1 + \bar{L}_1 \tag{A3}$$

$$Y_2(\rho) = H_2 + \bar{H}_2 + L_2 + \bar{L}_2 \tag{A4}$$

$$H_1(\rho) = E_4 L_1 + E_3 \bar{L}_1 \tag{A5}$$

$$H_2(\rho) = E_4 L_2 + E_3 \bar{L}_2 \tag{A6}$$

$$L_1(\rho) = \frac{1}{\Delta_2}\{(\kappa_1 + 1)\bar{Q}_1 - \bar{Q}_2\} \tag{A7}$$

$$L_2(\rho) = \frac{1}{\Delta_2}\{(\kappa_2 + 1)\bar{Q}_2 - \bar{Q}_1\} \tag{A8}$$

$$L_3(\rho) = \frac{e^{-\rho h}}{\Delta}\{(\bar{\gamma}_{11} + \cdots + \bar{\gamma}_{21}\} \tag{A9}$$

$$L_4(\rho) = \frac{e^{-\rho(h_1+h_2)}}{\Delta}\{(\gamma_{11} + \cdots + \bar{\gamma}_{21}\bar{\gamma}_{11})\} \tag{A10}$$

$$Q_1(\rho) = \bar{n}_1 L_3 + \bar{n}_2 \bar{L}_4 + n_3 \tag{A11}$$

$$Q_2(\rho) = l_1 L_3 + \bar{l}_2 \bar{L}_4 + l_3 \tag{A12}$$

$$\Delta_1(\rho) = Q_1 \bar{Q}_2 - Q_2 \bar{Q}_1 \tag{A13}$$

$$\gamma_{1k}(\rho) = \rho + (\kappa_1 + 1)\rho a_{1k} + \kappa_1 m_{1k} a_{1k}, \quad k = 1, \ldots, 4 \tag{A14}$$

$$\gamma_{2k}(\rho) = \kappa_1 m_{1k} + (\kappa_1 + 1)\rho - \rho a_{1k}, \quad k = 1, \ldots, 4 \tag{A15}$$

$$\Delta_2(\rho) = \gamma_{11}\bar{\gamma}_{21} - \bar{\gamma}_{11}\gamma_{21} \tag{A16}$$

$$A_1(\rho) = \frac{1}{\Delta_1}\{2(\kappa_1 + 1)\rho Y_1 - (\kappa_1 + 1)(1 + 2\rho)Y_2\} \tag{A17}$$

$$A_2(\rho) = \frac{1}{\Delta_1}\{2(\kappa_1 - (\kappa_1 + 1)\rho Z_2 + (\kappa_1 + 1)(1 - 2\rho Z_1)\} \tag{A18}$$

$$A_3(\rho) = \frac{1}{\Delta_1}\{2(\kappa_1 - 1)\rho Y_1 + (\kappa_1 + 1)(1 + 2\rho Y_2)\} \tag{A19}$$

$$A_4(\rho) = \frac{1}{\Delta_1}\{2(\kappa_1 - (\kappa_1 + 1)\rho Z_2 + (\kappa_1 + 1)(1 - 2\rho Z_1)\}. \tag{A20}$$

APPENDIX B

B.1. *Derivation of* $t_n(x)$

By letting $\alpha = -1/2, \beta = -1/2$ in the following recurrence relation for Jacobi polynomials (Abramowitz and Stegun, 1972)

$$(n+\alpha/2+\beta/2+1)(1+x)P_n^{(\alpha,\beta+1)}(x) = (n+\beta+1)P_n^{(\alpha,\beta)}(x) + (n+1)P_{n+1}^{(\alpha,\beta)}(x) \tag{B1}$$

we find

$$(1-x)P_n^{(1/2,-1/2)}(x) = P_n^{(-1/2,-1/2)}(x) + \frac{n+1}{n+\frac{1}{2}}P_{n+1}^{(-1/2,-1/2)}(x). \tag{B2}$$

From

$$P_n^{(-1/2,-1/2)}(x) = \frac{\Gamma(n+\frac{1}{2})}{n!\sqrt{\pi}}T_n(x) \tag{B3}$$

and eqn (B2) it follows that

$$(1-x)P_n^{(1/2,-1/2)}(x) = \frac{\Gamma(n+\frac{1}{2})}{n!\sqrt{\pi}}T_n(x) - \frac{n+1}{n+\frac{1}{2}}\frac{\Gamma(n+\frac{3}{2})}{(n+1)!\sqrt{\pi}}T_{n+1}(x),$$

$$= \frac{\Gamma(n+\frac{1}{2})}{n!\sqrt{\pi}}(T_n(x) - T_{n+1}(x)). \tag{B4}$$

Observing that $x = \cos\theta$ and

$$T_n(x) + T_{n+1}(x) = \cos(n\theta) + \cos(n+1)\theta = 2\cos(\theta/2)\cos(n+1/2)\theta, \tag{B5}$$

from eqn (B4) we obtain

$$P_n^{(1/2,-1/2)}(x) = \frac{\Gamma(n+\frac{1}{2})}{n!\sqrt{\pi}}\frac{\cos(n+1/2)\theta}{\cos(\theta/2)} = \frac{\Gamma(n+\frac{1}{2})}{n!\sqrt{\pi}}t_n(x), \tag{B6}$$

$$t_n(x) = \frac{T_n(x) - T_{n+1}(x)}{(1+x)}. \tag{B7}$$

B.2. *Some useful integrals involving Chebyshev polynomials*

$$\int_0^1 \sqrt{\frac{s}{1-s}}\,t_n(2s-1)\,ds = \begin{cases} \dfrac{1}{2n}\sin(2n\theta) - \dfrac{1}{2n+2}\sin(2n+2)\theta, & n \geqslant 1, \\ \theta + \frac{1}{2}\sin(2\theta), & n = 0, \end{cases} \tag{B8}$$

$$\int_0^1 s^2\sqrt{\frac{s}{1-s}}\,t_n(2s-1)\,ds = -\frac{1}{16}\left\{\frac{\sin(2n-4)\theta}{2n-4} + \frac{5\sin(2n-2)\theta}{2n-2} + \frac{5\sin(2n\theta)}{n} - \frac{10\sin(2n+2)\theta}{2n+2} + \frac{5\sin(2n+4)\theta}{2n+4} + \frac{\sin(2n+6)\theta}{2n+6}\right\}, \quad n \geqslant 3, \tag{B9}$$

$$= \frac{5}{8}\left(\frac{\pi}{2}-\theta\right) - \frac{1}{12}\cos^3\theta\sin\theta + \frac{5}{24}\cos^2\theta\sin\theta + \frac{5}{8}\cos\theta\sin\theta\Big\}, \quad n = 0 \tag{B10}$$

$$= \frac{5}{16}\left(\frac{\pi}{2}-\theta\right) - \left\{\frac{\sin 8\theta}{128} + \frac{5\sin 6\theta}{96} - \frac{5\sin 4\theta}{32} + \frac{11\sin 2\theta}{32}\right\}, \quad n = 1 \tag{B11}$$

$$= \frac{1}{16}\left(\frac{\pi}{2}-\theta\right) - \left\{\frac{\sin 10\theta}{160} + \frac{5\sin 8\theta}{128} - \frac{5\sin 6\theta}{48} + \frac{5\sin 4\theta}{32} + \frac{5\sin 2\theta}{32}\right\}, \quad n = 2 \tag{B12}$$

$$\int_0^1 \frac{sT_n(2s^2-1)}{\sqrt{s(1-s)}}\,ds = \begin{cases} \pi, & n=0, \\ \frac{\pi}{2}\cos n\theta, & n \text{ even}, \\ \frac{1}{2}\left\{\frac{\pi}{2}\cos n\theta - \frac{\sin 4\theta}{8}\sin 2\theta\right\}, & n=1, \\ \frac{1}{2}\left\{\frac{\sin(2n+2)\theta}{2n+2} - \frac{\sin(2n-2)\theta}{2n-2}\right\}, & n \geq 2, \end{cases} \tag{B13}$$

where

$$x = \cos^2\theta \tag{B14}$$

$$\frac{1}{\pi}\int_0^1 \frac{\ln|s-r|\,T_n(2s^2-1)}{\sqrt{s(1-s)}}\,ds = \begin{cases} 2\ln 2, & n=0, \\ \frac{1}{n}T_n(2r^2-1), & n \geq 1. \end{cases} \tag{B15}$$